Neogene volcanism of the Japan island arc: The K–h relationship revisited

Article · January 2008

CITATIONS
15

READS
524

2 authors:

Jun-Ichi Kimura
Japan Agency for Marine-Earth Science Technology
313 PUBLICATIONS **5,985** CITATIONS
SEE PROFILE

Bob Stern
University of Texas at Dallas
506 PUBLICATIONS **23,910** CITATIONS
SEE PROFILE

Arizona Geological Society Digest 22
2008

Neogene volcanism of the Japan island arc: The K-h relationship revisited

Jun-Ichi Kimura
Institute for Research on Earth Evolution (IFREE),
Japan Agency for Marine-Earth Science and Technology (JAMSTEC), Yokosuka 237-0061, Japan

Robert J. Stern
Geosciences Department, University of Texas at Dallas, Richardson, Texas, 75080-0321, USA

ABSTRACT

Japan is well suited for re-evaluating the K-h relationship (Dickinson and Hatherton, 1967), which summarizes enrichment of K and other LILEs as a function of depth (h) to the Wadati-Benioff Zone (WBZ). We use a newly-developed forward model – the Arc Basalt Simulator, or ABS – to isolate the most important controls on the K-h relationship for Neogene lavas from the Japan arc. Japan has endmember subduction zones, one subducting cold Cretaceous lithosphere rapidly (NE Japan or NEJ), the other subducting warm Neogene lithosphere slowly (SW Japan or SWJ). Modern geochemical data indicates different but nearly parallel K-h relationships. The NEJ K-h relationship follows the global curve of Dickinson and Hatherton (1967) but K-h for SWJ defines greater K for given h. Other incompatible trace element concentrations reflect this as well. The basalts erupted along the SWJ magmatic front are similar to those from the NEJ rear arc, reflecting a fundamental difference between the two subduction zones as is also indicated by the presence of adakites (slab melts) in SWJ and their absence in NEJ. The subducted slab beneath SWJ is much hotter than that beneath NEJ, resulting in an order of magnitude less melt generation. ABS modeling suggests that these differences are controlled by different extents of slab hydration, with the colder oceanic crust and perhaps mantle peridotite carrying much more water deep into the NEJ subduction zone than does the hot, relatively dry SWJ subducted slab. The greater water flux beneath NEJ results in a greater degree of mantle melting beneath the magmatic front of NEJ (20% melting) compared to SWJ (3-5% melting). Because the lithosphere subducted beneath SWJ slab is younger and hotter, it carries less water to depths in the mantle where it can trigger melting, because it is less hydrated and/or loses its water shallower. We conclude that the K-h relationship for NEJ, SWJ, and perhaps global arcs is controlled by the thermal state of the subducted slab, which controls fluid flux to and extent of melting of asthenosphere in the mantle wedge, and thus K (and other incompatible element) contents.

INTRODUCTION

Even before the K-h relationship was first proposed in 1967 (Dickinson and Hatherton, 1967), controls on the composition of arc magmas have been the center of petrologic and geochemical interest (Coats, 1962; Kuno, 1966). The K-h relationship is the positive correlation between the geophysically-inferred depth (h, in kilometers of the subducted slab surface (Wadati-Benioff Zone; WBZ) with K (K_2O wt.%) of lavas normalized at SiO_2 = 55 or 57.5 wt.% (K_{55} or $K_{57.5}$).

e-mail: Kimura: jkimura@jamstec.go.jp; Stern: rjstern@utdallas.edu

Kimura, J.-I., and Stern, R.J., 2008, Neogene volcanism of the Japan island arc: The K-h relationship revisited, *in* Spencer, J.E., and Titley, S.R., eds., Ores and orogenesis: Circum-Pacific tectonics, geologic evolution, and ore deposits: Arizona Geological Society Digest 22, p. 187-202.

Such spatial variations in lava chemistry appear a fundamental feature of convergent margin magmatism, observed for both Andean-type (continental) as well as truly intra-oceanic arcs (Aramaki and Ui, 1982; Dickinson, 1975; Hatherton and Dickinson, 1969; Hutchison, 1982). These and other studies hint that a fundamental tectonomagmatic process in the subduction zone is responsible the K-h relationship. For this reason, a better understanding of what controls the K-h relationship opens a door to understanding subduction zone processes.

In this paper we investigate controls on the K-h relationship, using late Neogene lavas from the Japan island arc. The Japan arc is a natural focus of such studies, because numerous studies by especially Japanese scientists results in a detailed understanding of its tectonic setting, subduction zone geometry, and magmatic compositions. Japan is actually the site of three arc segments: NE Japan (NEJ), SW Japan (SWJ), and Izu-Bonin-Mariana (IBM), which meet at Earth's only T-T-T triple junction (Fig. 1). We focus on NEJ and SWJ arcs because their very different magmatic systems are associated with very different convergence rates and subduction zone thermal regimes. NEJ subducts old, cold lithosphere rapidly, whereas SWJ subducts young, hot lithosphere slowly (Kimura et al., 2005; Kimura and Yoshida, 2006; Nakajima and Hasegawa, 2007; Peacock, 1996). The two contrasting arcs are also well suited to this treatment because they are so different and so well known (Nakajima and Hasegawa, 2007; Nakajima et al., 2005). Thermal structure and fluid transfer in the subducting slab and wedge mantle are well-constrained by both geodynamic (Furukawa, 1993; Peacock et al., 2005; van Keken et al., 2002) and petrological/geophysical models (Hacker and Abers, 2004; Hacker et al., 2003; Iwamori, 1998; Poli and Schmidt, 1995). We build on this knowledge to understand the K-h relationship by applying the simple Arc Basalt Simulator (ABS) model (Kimura and Yoshida, 2006; Sendjaja et al., in press). ABS presents a simplified, realistic magma genetic model that incorporates intensive and extensive parameters during slab dehydration, fluid-mantle reaction, and peridotite partial melting processes (Sendjaja et al., in press). A geochemical database for Japanese lavas (Kimura et al., 2005; Kimura and Yoshida, 2006) allows us to apply the ABS model. Here we present the results of our analysis, which allow us to conclude that the K-h relationship reflects temperature-dependent slab dehydration and subsequent mantle melting controlled by the amount of slab fluid added to the mantle wedge. These affects are most strongly controlled by the thermal structure of the subducted slab and to a lesser extent by the mantle wedge.

SUBDUCTION ZONES AND MAGMATIC ARCS OF JAPAN

The Japanese islands form a complex arc system with five volcanic arcs on three different plates developed in response to subduction of the Pacific plate beneath the Eurasian plate to form the Kurile and Northeast Japan (NEJ) arcs, the Pacific plate beneath the Philippine Sea plate to produce the Izu-Bonin-Mariana (IBM) arcs, and the Philippine Sea plate beneath the Eurasia plate to produce the Southwest Japan (SWJ) and Ryukyu arcs (Fig. 1a; Nakajima and Hasegawa, 2007). The Pacific plate is the oldest plate in the world (> 160 Ma), with a WBZ that can be traced to > 500 km deep (Nakanishi et al., 1992). The WBZ of the Philippine Sea plate is inserted between the subducted Pacific plate and the surface Eurasian plate to form the SWJ arc. Most of the Philippine Sea plate subducting beneath SWJ is lithosphere of the Shikoku Basin, which formed 27-15 Ma ago by back arc basin spreading of the IBM arc (Okino et al., 1994). Earth's only T-T-T triple junction lies where the NEJ-SWJ-IBM arcs meet; here the IBM arc collides end-on with the Eurasia plate (Fig. 1a). The NEJ volcanic arc thus reflects the subduction of the old and cold Pacific plate, whereas the SWJ arc reflects the subduction of the young and hot Philippine Sea plate.

Northeast Japan (NEJ) arc

The old, cold Pacific plate dips beneath the Eurasia plate at 20-30° and the NEJ trench-magmatic front gap is about 300-km wide (Hasegawa et al., 1991). NEJ is classified as an erosive margin (Clift and Vannucchi, 2004; von Huene and Scholl, 1991). Subducted sediment and oceanic crust thicknesses are estimated from seismic profiles to be 0.5-1 km (Tsuru et al., 2002) and 7-8 km (Miura et al., 2005) respectively. The Pacific plate subducts at ~10 cm/y (Seno et al., 1993). The NEJ volcanic arc lies ~120 to ~220 km above the WBZ (Fig. 1b). The great density of seismic stations in Japan and abundant seismicity in the down-going Pacific plate combine to allow excellent tomographic imaging of the mantle wedge. A sheet-like zone with low-Vp and -Vs is developed in the mantle wedge parallel to the subducted slab, and the shallow part of the zone rises to the Moho beneath the volcanic front. This is interpreted to be a partially molten zone in the mantle wedge (Hasegawa et al., 1991; Nakajima et al., 2005).

The NEJ volcanic arc is about 200-km wide with more than 48 volcanoes that have been active during the Quaternary (Fig. 1b). Two rows of volcanoes define volcanic front and rear arc arrays, which erupt low- to medium-K and high-K (Gill, 1981) suite lavas, respectively (Kimura and Yoshida, 2006). This geochemical variation was established at about 0.8 Ma by addition of the rear arc high-K suite to a medium- to low-K volcanic front suite, which was active since 2 Ma (Kimura and Yoshida, 2006). Magma eruption rate over the past 2 million years is 2.11 km^3/Myr/km (cubic kilometer per million years for each kilometer arc length), with 1.94 km^3/Myr/km for the volcanic front and 0.17 km^3/Myr/km for the rear arc (Kimura and Yoshida, 2005). Greater magma production beneath the volcanic front is common for arcs (Tatsumi and Eggins, 1995).

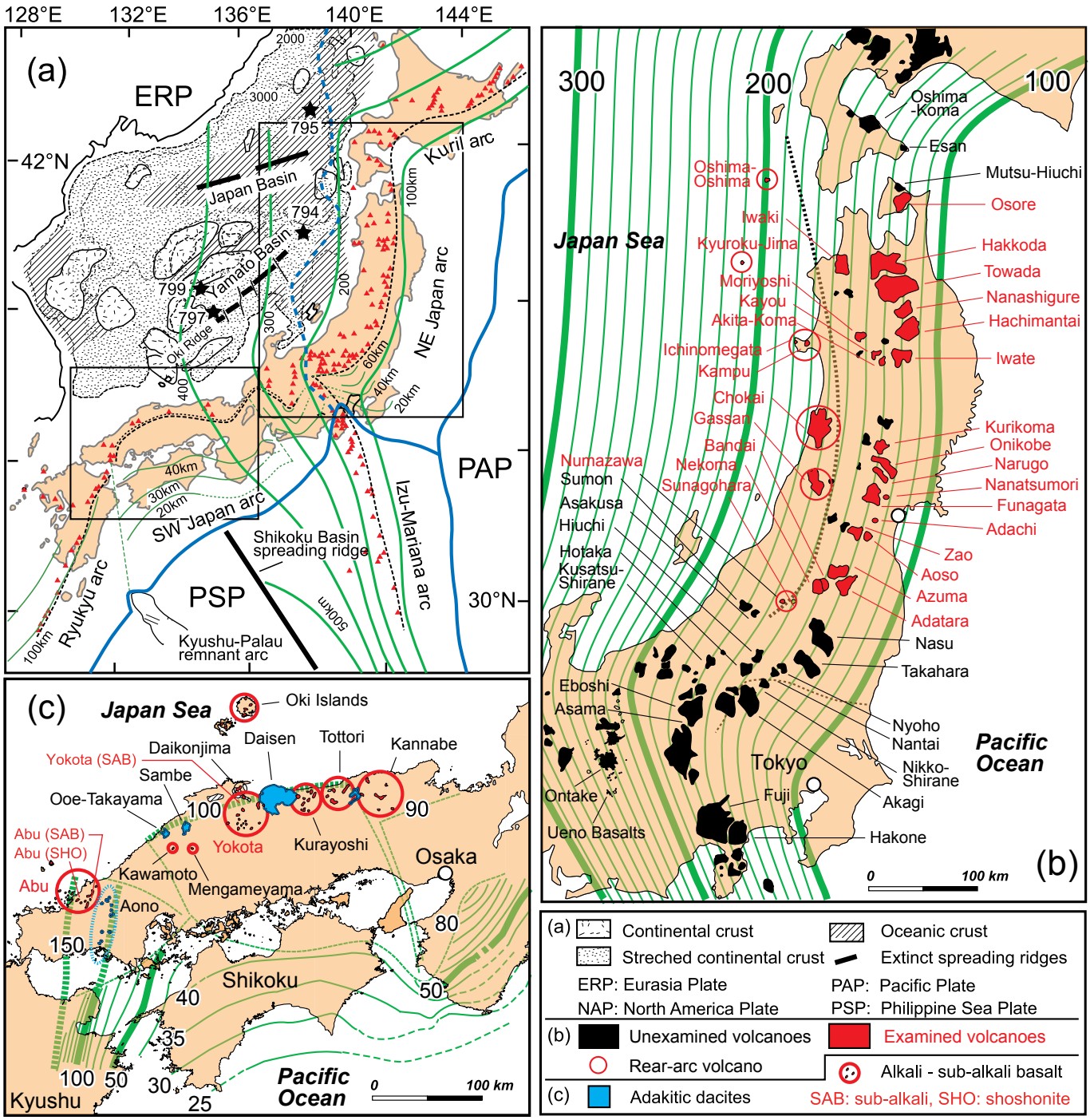

Figure 1. Tectonic setting and distribution of volcanoes in arcs in and around Japan. Green lines indicate depth to the top of Wadati-Benioff zone. Dashed line indicates position of magmatic front. Numbered stars indicate ODP drillsites in Sea of Japan. (a) Tectonic configurations of the Japanese arc system. (b) Distribution of Quaternary volcanoes and depth of the Wadati-Benioff Zone for NE Japan arc. (c) Distribution of the Quaternary volcanoes and depth of the Philippine Sea plate slab surface for SW Japan.

Southwest Japan (SWJ) arc

The SWJ volcanic arc formed by subduction of the Philippine Sea plate (PSP) (Okino et al., 1994; Fig. 1c). The shape of the PSP beneath SWJ is complex. To the east, the Izu arc crust collides with Japan and the Shikoku Basin subducts at various angles. The subduction angle varies from almost vertical through 40° to about 25°. The shallowest dipping slab underlies Shikoku and the Setouchi Inland Sea (Kimura et al., 2005; Nakajima and Hasegawa, 2007; Fig. 1c). The subduction angle steepens again, > 60° to vertical, to the west beneath Kyushu and farther SW beneath the Ryukyu arc (Fig. 1a). This

variation in subduction zone dip reflects different ages of the PSP seafloor, younger (15-27 Ma) in the Shikoku Basin, older (> 27 Ma up to 60 Ma) west of the Kyushu-Palau remnant arc. Shikoku Basin lithosphere began to subduct beneath SWJ at 15 Ma (Kimura et al., 2005; Kimura and Yoshida, 2006; Seno et al., 1993). Therefore, subducted PSP slab would have been quite hot and buoyant beneath the central segment of SWJ, leading to shallow angle subduction (Stern, 2002).

Subduction of the youngest part of the Shikoku Basin occurs at the Nankai Trough at a rate of ~4 cm/y (Seno et al., 1993). Sediments approaching the trench are 1.8 to 3.2 km thick, whereas oceanic crust is 5.0-6.3 km thick (Kodaira et al., 2002). The sediment thickness is much greater than for the Pacific plate subducting beneath NEJ, whereas the oceanic crust is somewhat thinner than that for NEJ or the global average (7.1±0.8 km (White et al., 1992)). A thick accretionary prism is developed in the Nankai subduction zone, and this prism consists of terrigeneous sediments and accreted oceanic crust materials (Kodaira et al., 2002; Taira, 2001). Structure of the SWJ mantle wedge has been examined using seismic tomography (Nakajima and Hasegawa, 2007; Ochi et al., 2001). The aseismic Shikoku Basin segment of the Philippine Sea plate is shallower beneath the volcanic arc in the central part of SWJ where its depth is about 70-100 km as revealed by seismic tomography (Nakajima and Hasegawa, 2007). However, the leading edge of the slab is not well constrained (Nakajima and Hasegawa, 2007; Ochi et al., 2001).

The present Southwest Japan volcanic arc was established at ~3 Ma. The magmatic arc is narrow, usually less than 50 km wide (Kimura et al., 2003). The Plio-Pleistocene lavas consist of intra plate-type alkali basalt and adakitic dacite with trace amounts of alkali to sub-alkali basalt having arc signatures (Kimura et al., 2003; Kimura et al., 2005). These geochemical features indicates that melting of hot and young Shikoku Basin slab occurs beneath the central SWJ arc (Kimura et al., 2003; Kimura et al., 2005; Morris, 1995; Peacock and Wang, 1999). The young Shikoku Basin plate subducts only beneath the central SWJ arc, but older Philippine Sea plate slab subducts beneath Kyushu although the transition between the two is not clearly defined beneath SWJ (Fig. 1). Distribution of the adakitic dacite is limited within this central segment including the transition region to Kyushu around Aono-Abu volcanoes (Fig. 1). Therefore, we take this segment as a typical young subduction zone. Quaternary lavas mostly define medium-K to high-K suites. Shoshonitic lavas occur in the Abu region. Low-K Quaternary lavas are not present in the SWJ arc (Kimura et al., 2005).

K-h relationship for the NEJ and SWJ arcs

The K-h relationship (Dickinson, 1975; Dickinson and Hatherton, 1967) for the NEJ and SWJ arcs was examined by calculating $K_{57.5}$ (regressed K_2O wt.% at SiO_2 = 57.5 wt.%) for each Quaternary volcano. Linear regressions were applied to calculate $K_{57.5}$ whenever the lavas contained at least 57.5 wt.% SiO_2 ; if not, regression lines formed by lava compositions were extrapolated to 57.5% SiO_2 by examining the parallelism to the general fractionation trend (Gill, 1981). $K_{57.5}$ for the Setouchi high-magnesium andesite (HMA) of middle Miocene age (~12 Ma) (Tatsumi et al., 2001) in the SWJ arc were also calculated using the present WBZ depth of 60 km (Fig. 2; HMA are not discussed further below).

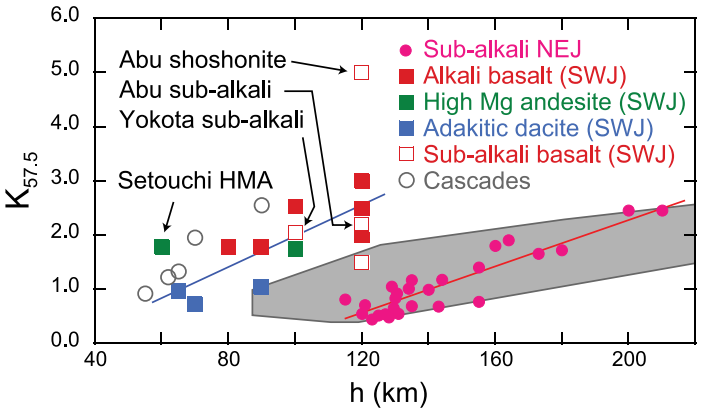

Figure 2. K-h relationship for NE Japan and SW Japan arc lavas. Grey shaded area: K-h global trend (Dickinson, 1975).

The NEJ Quaternary lavas show a linear K-h relationship with $K_{57.5}$ = 0.5 wt.% at h = 120 km and $K_{57.5}$ = 2.5 wt.% at h = 200 km. This overlaps the global K-h trend (Dickinson, 1975; Fig. 2). However, the K-h slope of the NEJ lavas define slightly steeper slope than that formed by the global trend. This may be due to improvement of seismological observations and growth of geochemical database since the first compilation was made, or due to characteristics of the NEJ arc (Gill, 1981).

In contrast to NEJ lavas, SWJ lavas have extremely high K for a given slab depth. Due to poor definition of the WBZ beneath SWJ, slab depth is estimated by extrapolating the top surface of the high-*Vp*, high-*Vs* tomographic regions in the mantle wedge (Nakajima and Hasegawa, 2007). Although the slab depth is poorly defied, the elevated K-h relation in the SWJ should be real because of the existence of geochemical arc signatures in the Quaternary adakites (Tottori (< 1.7 Ma), Daisen (< 1 Ma), Sambe (< 1.5 Ma), Ooe-Takayama (< 1.8 Ma), and Aono (< 1.2 Ma) volcanoes; see Fig. 1c) and sub-alkali (Yokota (< 2.4 Ma) and Abu (< 1.7 Ma) volcanoes; Fig. 1c) and some alkali basalt (Yokota and Abu) lavas with arc signatures erupted above where aseismic slab is believed to exist, which suggests input of slab component into the magma source (Kimura et al., 2003; Kimura et al., 2005). The results show a broad positive correlation in K-h, $K_{57.5}$ = 1 wt.% at h = 60 km and $K_{57.5}$ = 2.5 wt.% at h = 120 km, with considerable scatter (Fig. 2). A shoshonite suite with $K_{57.5}$ = 5 wt.% occurs at 120 km above the slab, emphasizing the scatter. Compared to the "normal" NEJ arc lavas, the slab depth that correlates with medium-K lavas in the SWJ arc is about half that for NEJ

(120 km in NEJ vs. 60 km in SWJ). The high-K suite in the SWJ occurs at h = 120 km, contrasting with its occurrence at h = 200 km for NEJ (Fig. 2). The high K content of SWJ arc lavas is further emphasized by the fact that $K_{57.5}$ in some of analyzed samples from the SWJ magmatic front are similar that for NEJ rear arc lavas.

A similar compilation for the southern Washington Cascade lavas (GEOROC, 2007; Fig. 2) overlaps with the SWJ arc lavas. Cascade arc volcanism is the result of slow (< 4 cm/y) subduction of the young (< 10 Ma) Juan de Fuca oceanic plate (Leeman et al., 2005), and thus, has a similar tectonic setting to that of SWJ. This supports the interpretation that the unusually high $K_{57.5}$ of SWJ is not just anomalous but is found for other arcs subducting young crust.

Covariation of fluid mobile elements with K

High quality incompatible trace element data has become available (GEOROC, 2007) since the original K-h relationship was articulated 40 years ago. There is considerable covariation between K and other incompatible trace elements. Extended trace element plots of representative NEJ rear arc basalts indicate systematic enrichment of all incompatible trace elements relative to NEJ volcanic front basalt. Enrichment is greater with increasing incompatibility of the elements (Fig. 3). Contents of Th, U, and light rare earth element (LREE) smoothly decrease from 10 times contents in volcanic front basalt to about the same for heavy (H)REE (Fig. 3). Exceptions are Ba, Nb, Ta, Pb, and Sr, which all show negative spikes relative to neighboring elements. Rb and K are enriched relative to neighboring elements (Fig. 3). If the smoothly inclined slope is attributed to different degrees of partial melting in the mantle source (Sakuyama and Nesbitt, 1983), then the deficits in Ba, Nb, Ta, Pb, and Sr, and excess Rb and K in rear arc basalts may be due to different slab fluid (or melt) compositions (Pearce, 2005; Pearce and Parkinson, 1993). If the behavior of incompatible trace elements is any guide, the K-h relationship appears to be controlled both by degree of partial melting and by different fluids (melt) supplied beneath the regions (Kimura and Yoshida, 2006).

It is very interesting that sub-alkali high-K basalts from SWJ (Yokota volcano) erupted at h = 80-120 km are chemically indistinguishable from NEJ rear arc basalts erupted at h = 160-200 km (Fig. 3). This implies that the slab fluid (melt) composition and melting degree of the source mantle peridotite was similar beneath the SWJ magmatic front and the NEJ rear arc in spite of very different slab depths. Although adakite, HMA, and intra plate-type alkali basalt are major components of SWJ lavas they are not suitable for broad comparison because of their different genetic mechanisms; e.g., slab melting and subsequent reaction of the melt with mantle peridotite (adakite and HMA) or mantle melting without slab fluxes (intra plate-type alkali basalt) (Kimura et al., 2005; Morris, 1995; Shimoda et al., 1998; Tatsumi and Hanyu, 2003). These are not discussed further below.

Arc Basalt Simulator model

The Arc Basalt Simulator (ABS) is a model which simulates; 1) slab fluid dehydration; 2) fluid-mantle reaction; and 3) fluid-fluxed mantle melting (Sendjaja et al., in press). This model uses experimentally-determined temperature-pressure dependent distribution coefficients between slab and fluid (Kessel et al., 2005a) to calculate the composition of fluid

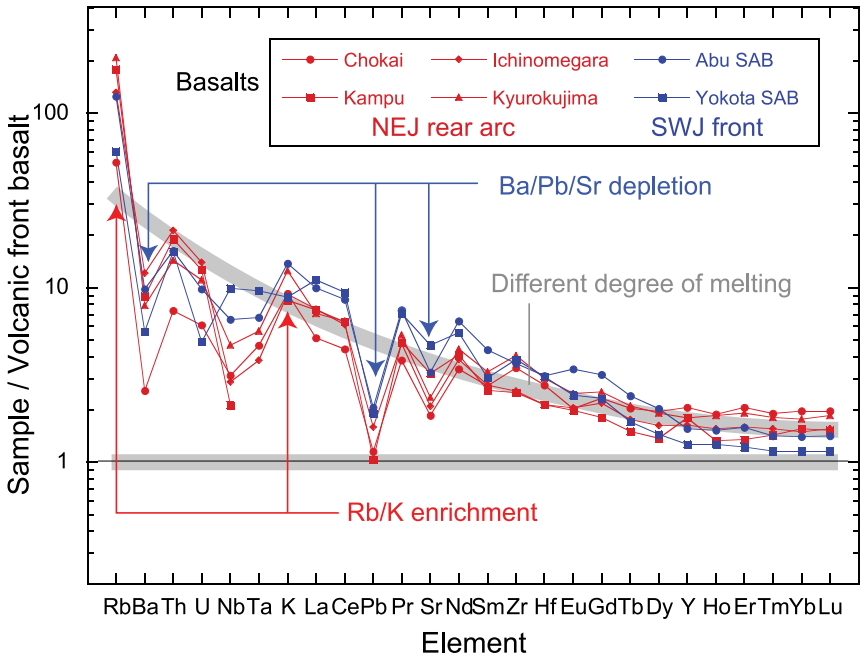

Figure 3. Primary basalt compositions for NEJ rear arc and SWJ magmatic front volcanoes normalized against typical NEJ volcanic front basalt. Estimated Funagata primary basalt composition (Kimura and Yoshida, 2005) is used for normalization (denominator of the vertical axis). Flat, thick, shaded lines: NEJ volcanic front basalt; inclined shaded line: approximate melt composition generated by lower degree of melting (F = 3 %) from the volcanic front basalt source.

released by the subducted crust and sediments, zone refining reaction between slab-generated fluid and mantle peridotite (Ayers, 1998), and open system, fluid-fluxed dynamic melting (Ozawa and Shimizu, 1995; Zou, 1998, 1999) for generating the trace element and isotopic composition of arc basalt magma (Sendjaja et al., in press). All the parameters that define the three reactions are intensive or extensive variables, including; 1) temperature (T_{slab}) and pressure (P_{slab}) where slab dehydration occurs; 2) mass of mantle peridotite that reacts with fluid at (n) times fluid mass in zone refining reaction; and 3) fluid fluxed rate against melt mass (β), pressure (P_{melt}) and degree of melting (F) where mantle melting occurs. Iterative fitting using AOC (X_{AOC}), SED (X_{SED}), and PERID (X_{PERID}) source compositions and target basalt composition (X_{BAS}) is available for 24 incompatible trace elements and K, and Sr-Nd-Pb isotopic compositions (Sendjaja et al., in press). The ABS model is particularly useful because, when a reasonable fit is obtained between real and modeled basalt compositions, ABS results yield information about slab and mantle wedge conditions that are otherwise very difficult to obtain. This program file is Microsoft™ EXCEL®-based and is available by contacting JIK.

Although slab fluid (or melt) compositions and degree of partial melting of mantle peridotite appear to be similar for the NEJ rear arc and SWJ magmatic front, the subducting sediment composition between the arcs are different. Thinner sediments with a higher pelagic component is subducted beneath NEJ, whereas a thicker section of more terrigeneous sediments at least partly subducted beneath SWJ (Plank and Langmuir, 1998; Shimoda et al., 1998). Altered oceanic crust subducted beneath the two arcs is also different isotopically. Subducted Pacific plate oceanic crust was generated from Pacific domain mantle, whereas that of the Shikoku Basin (PSP) was generated from the Indian Ocean mantle domain (Hauff et al., 2003; Hickey-Vargas, 1991; Kelley et al., 2003). Mantle wedge peridotite compositions should also be different in terms of isotopic compositions, more depleted beneath NEJ (Kimura et al., 2005; Kimura and Yoshida, 2006; Shibata and Nakamura, 1997) and relatively fertile beneath SWJ (Hoang and Uto, 2003; Kimura et al., 2001; Shimoda et al., 1998; Tatsumi and Hanyu, 2003). Without taking these differences into account, comparison of the intensive (degree of melting) and extensive (slab fluid composition) parameters may lead to misleading conclusions regarding the origin of the K-h relationship for the two Japanese arcs.

Controlling factors of fluid mobile element enrichment

We applied the ABS model to NEJ magmatic front and rear arc basalts and to SWJ sub-alkali (Yokota) and shoshonite (Abu) basalts. The model used ODP 579 sediment for the Pacific Plate (Plank and Langmuir, 1998) and ODP 801/1149 AOC composition (Hauff et al., 2003; Kelley et al., 2003) for NEJ subducted inputs and ODP 808 Nankai Trough sediment (Plank and Langmuir, 1998) and combined ODP 801/1149 trace element composition and typical Shikoku Basin MORB isotopic compositions (Hickey-Vargas, 1998; Hickey-Vargas et al., 1995) for AOC of the SWJ subducted slab. Mantle peridotite trace element compositions were estimated by melt depletion at various degrees from primitive mantle (Sun and McDonough, 1989) calculated by ABS (Sendjaja et al., in press). Isotopic composition of the mantle sources were estimated from Japan Sea basalts for NEJ (Kimura and Yoshida, 2006) and from the intra plate-type alkali basalts for SWJ (Hoang and Uto, 2003; Shimoda et al., 1998; Tatsumi and Hanyu, 2003). These trace element and isotope compositions are listed in Table 1 and shown in Figs. 4 and 5. Partition coefficients and other melting parameters are based on the ABS model (Sendjaja et al., in press).

The ABS results reasonably reproduce the trace element and Sr-Nd-Pb isotope compositions of NEJ volcanic front and rear arc basalts except for elevated Rb and K contents and a slight deficit in Sr for volcanic front basalt (Fig. 4). Modeled SWJ sub-alkali basalt also has elevated K and Rb relative to natural lavas (Fig. 4). Using the same source materials, modeled SWJ shoshonite lava fit with K and Rb contents, although with slightly low Pb, Ba, and Th contents (Fig. 4). The large discrepancies in K and Rb between the ABS model results and natural basalts are largely attributable to the lack of consideration of sheet silicates in residual slab or mantle (biotite, phengite, and phlogopite) in the model (Sendjaja et al., in press). Isotopic compositions of NEJ and SWJ basalts are also reasonably reproduced, although source X_{AOC}, X_{SED}, X_{PERID} differ greatly between the arcs (Fig. 5). Mantle source compositions used are 4% depleted (NEJ) and 0.5% depleted mantle (SWJ) (Fig. 4). The greater trace-element depletion for the NEJ arc rocks is reasonable because of depleted isotopic compositions in Sr and Pb with enriched Nd isotope composition (Fig. 5).

Origin of the K-h relationship: Examination with ABS model

The origin of the K-h relationship has been extensively discussed, using the higher quality and more comprehensive trace element and isotopic datasets that now exist, but no consensus on what is the most important control has been reached. There are a wide range of explanations, which include: 1) Greater fluid addition to the mantle beneath the magmatic front than beneath the rear arc (Ishikawa and Nakamura, 1994; Ishikawa and Tera, 1999; Moriguti et al., 2004; Shibata and Nakamura, 1997). Lower fluid flux would result in lower degrees of mantle melting beneath the rear arc, so causing the K-h relationship (Sakuyama and Nesbitt, 1983); 2) Different mineral stabilities at different slab pressure may yield different slab-derived fluid compositions and thus control across-arc geochemical variations (Pearce and Parkinson, 1993; Pearce and Peate, 1995; Pearce et al., 2005); 3) Differential hydrous fluids progressively squeezed and sweated from altered oceanic crust or sediments added to the region of melting in mantle wedge

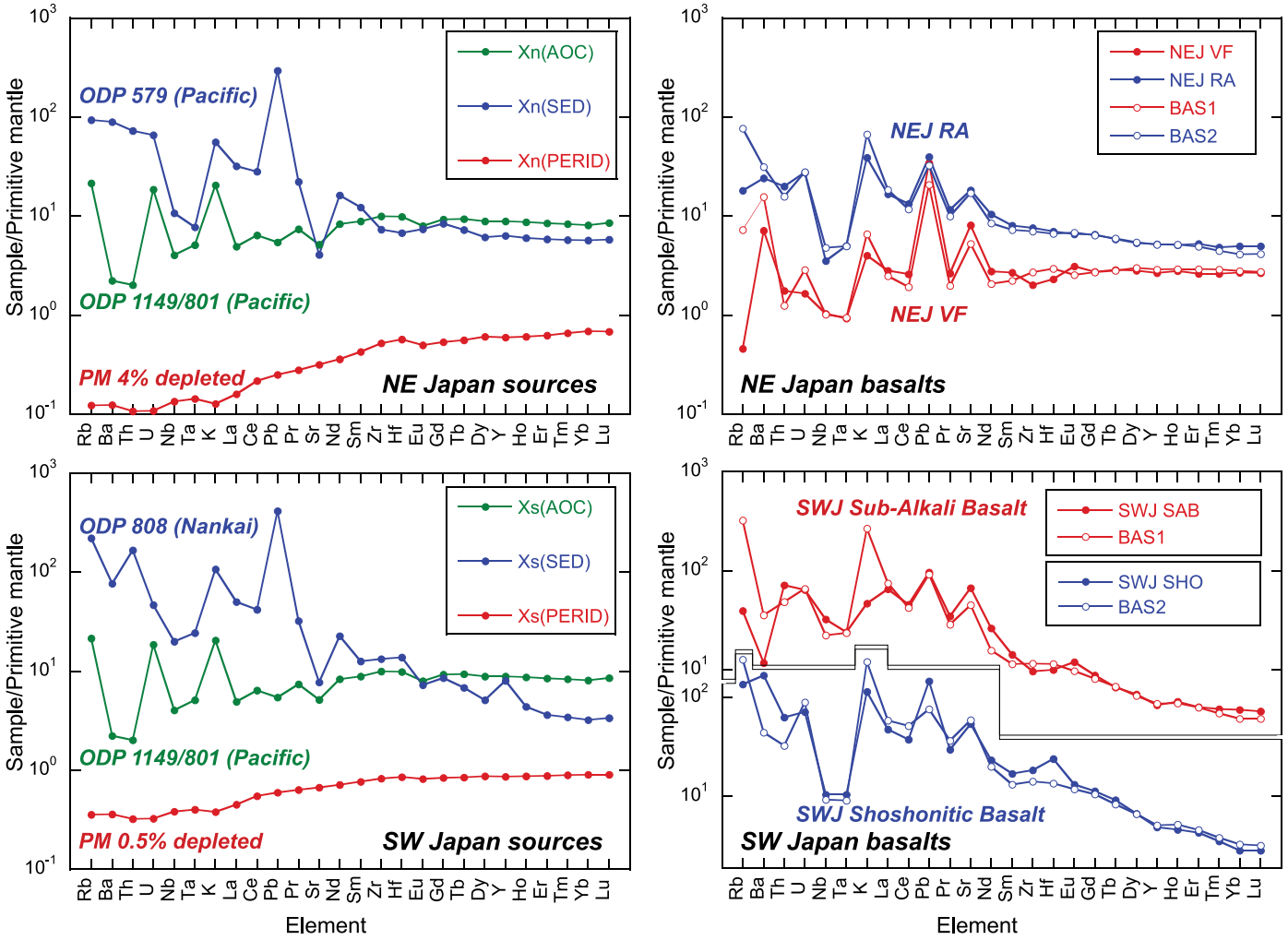

Figure 4. Primitive mantle-normalized incompatible element compositions for ABS model inputs and outputs and typical NEJ and SWJ lavas. Left panels: sediment (SED), altered oceanic crust (AOC), and peridotite (PERID) sources for the NEJ (upper) and SWJ (lower) arc basalts. Right panels: comparison between natural primitive basalts (NEJ VF, NEJ RA, SWJ SAB, SWJ SHO) and ABS model (BAS1, BAS2) for NEJ (upper) and SWJ (lower) lavas. VF: volcanic front, RA: rear arc, SAB: sub-alkali basalt, SHO: shoshonite. Note that chemical composition for ODP 801/1149 AOC is used for both NEJ and SWJ subduction AOC input, whereas different isotopic compositions are used for AOC in Figure 5.

(Ishizuka et al., 2003; Ishizuka et al., 2006); 4) Pressure dependent breakdown of phlogopite in mantle peridotite may yield K-rich (shoshonitic) lava in the rear arc (Edwards et al., 1991; Tamura et al., 2007; Tatsumi and Eggins, 1995); and 5) More complex models, including multiple enrichment-metasomatism-melt extraction events in the wedge mantle (Hochstaedter et al., 2001) or pre-conditioning of the mantle source by melt interaction (Pearce, 2005). Such models may explain lateral K variations in arc lava compositions, but have greater difficulties explaining K-h.

Modeling of NEJ and SWJ arc lavas using ABS allows a new perspective on the K-h relationship. The intensive and extensive parameters for the ABS model are summarized in Table 2. Pressures (4-6 GPa = ~120-180 km depth) estimated for slab dehydration are generally consistent with the depth of the WBZ beneath the volcanoes examined. Pressure of 4 GPa (~120 km) is estimated for NEJ VF basalt and SWJ-SAB on the volcanic front, whereas 6 GPa (~180 km) is estimated for NEJ RA and 5 GPa (~150 km) for Abu shoshonite. As shown in Fig. 1b, the NEJ VF and NEJ RA volcanoes lie above ~120 km and 160-180 km depth contours of the WBZ, respectively. The SWJ-SAB (Yokota) lies above ~100 km and SWJ-SAB (Abu) is on ~130 km, whereas SWJ-SHO lies at ~140 km, respectively (Fig. 1c), generally consistent with the pressure estimates used by the ABS model. Other parameters, including degree of melting, fluid flux rate (~H_2O in primary basalt), and depths of mantle fluxed melting, are within reasonable range for arc basalt genesis (Kimura and Yoshida, 2006).

At high temperatures expected for the slab interface beneath the NEJ RA (T_{slab} = 1020 °C) and SWJ-SAB (T_{slab} =

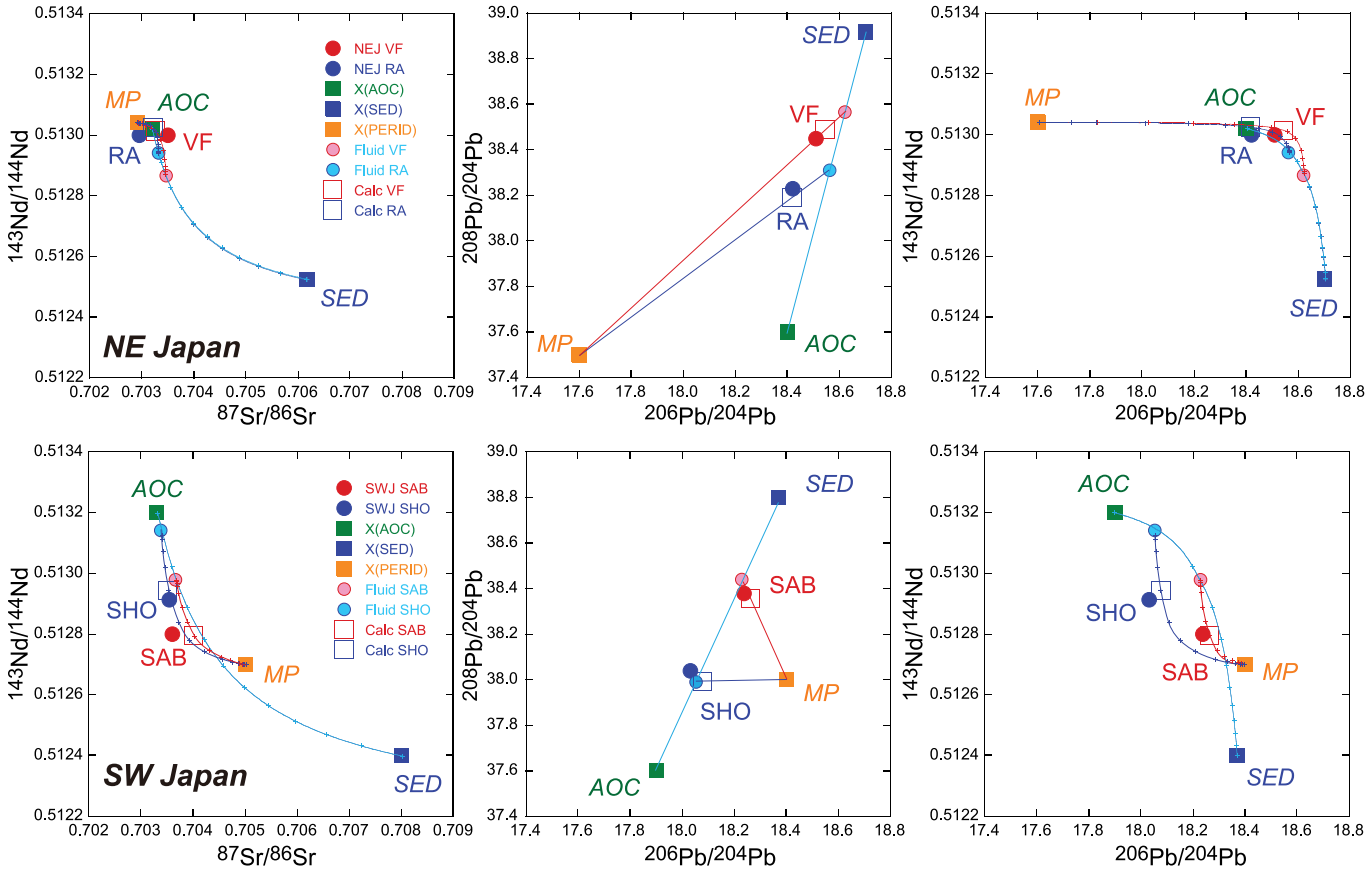

Figure 5. Isotopic compositions of natural and ABS modeled basalt and source compositions. SED: sediment, AOC: altered oceanic crust, MP: mantle peridotite. VF: volcanic front basalt, RA: rear arc basalt, SAB: sub-alkali basalt, SHO: shoshonite natural lava compositions. Upper panels: NEJ arc, lower panels: SWJ arc.

1050 °C), and SWJ shoshonite (T_{slab} = 1050 °C), partial melting of the slab should occur. This is confirmed by experiments (Kessel et al., 2005a; Kessel et al., 2005b). However, slab melting generates felsic melts which may not be able to reach the surface without extensive reaction with the mantle wedge due to high dihedral angle against mantle olivine (Maumus et al., 2004). Co-existing adakite and HMA suggest slab melts are involved in magma genesis beneath SWJ; however, the examination given here is limited to basalts. In fact, SWJ basalt volcanism did not coincide temporally or spatially with adakite or HMA volcanism (Kimura et al., 2003; Kimura et al., 2005). Furthermore fluid-solid partition coefficients used in ABS were originally determined by a diamond trap method, although partial melts coexisted in high temperature experiments (Kessel et al., 2005a; Kessel et al., 2005b). Therefore, the approach below is supported by the reasonable assumption that the basalts in the two arcs were generated by mantle peridotite melting due to slab-fluid fluxing.

Here we examine various causes of the K-h relationship for SWJ and NEJ, using the ABS results. Conditions examined are 1) mineralogy, 2) slab source composition, 3) slab dehydration parameters, 4) fluid flux rate, and 5) degree of mantle melting.

DO SPECIFIC MINERALS CONTROL K-h? – YES, TO A LIMITED EXTENT

Specific sheet silicates in the fluid source regions, such as biotite, phlogopite or phengite, can control K contents in basalt (Tamura et al., 2007). However, these minerals do not control other incompatible elements due to low partition coefficients (Green and Adam, 2003). Therefore, 1) the overall fit of the 24 trace elements and Sr, Nd, and Pb isotope compositions by the ABS model and 2) the co-variation of K with other incompatible elements negates the possibility that sheet silicate equilibria alone is responsible for the K-h relationship. Amphiboles can control K along with HREE due to high partition coefficients for these elements (Green, 1994; Tiepolo et al., 2000). However, very low partition coefficients for LREEs results in an absence of covariation between K and LREE, which negates the possibility that amphibole equilibria alone is responsible for the K-h relationship.

The ABS model does not consider minor phases as noted above (Kimura and Yoshida, 2006; Sendjaja et al., in press). Significant discrepancies exist in highly fluid-mobile Rb and K between the ABS results and natural basalts (Fig. 4). Partial control by micas and amphiboles may occur as these minerals

TABLE 1: SOURCE COMPOSITIONS AND PRIMITIVE BASALT COMPOSITIONS USED FOR THE ABS MODEL CALCULATIONS

Element	NEJ VF	NEJ RA	Xn(AOC)	Xn(SED)	Xn(PERID)	SWJ SAB	SWJ SHO	Xs(AOC)	Xs(SED)	Xs(PERID)
Rb	0.294	11.500	13.700	59.900	0.100	25.113	86.800	13.700	140.865	0.228
Ba	50.100	170.000	15.600	627.404	1.111	82.406	1172.07	15.600	540.093	2.525
Th	0.150	1.710	0.173	6.217	0.012	6.113	5.363	0.173	14.200	0.027
U	0.035	0.585	0.390	1.389	0.003	1.358	1.503	0.390	0.985	0.007
Nb	0.737	2.520	2.890	7.670	0.123	23.150	7.460	2.890	14.315	0.273
Ta	0.038	0.207	0.210	0.319	0.008	0.981	0.428	0.210	1.008	0.016
K	1003.0	9835.0	5146.9	14073.8	41.5	11725.8	28749.7	5146.9	26882.8	95.2
La	1.950	11.500	3.400	21.938	0.142	44.925	32.952	3.400	34.700	0.310
Ce	4.630	23.800	11.400	50.108	0.494	81.288	66.864	11.400	74.850	0.979
Pb	2.770	3.200	0.437	23.682	0.025	7.770	11.704	0.437	33.370	0.048
Pr	0.731	3.230	2.060	6.141	0.097	9.650	8.232	2.060	8.967	0.176
Sr	172.000	386.000	109.000	86.615	8.266	1423.53	1149.87	109.000	164.557	14.246
Nd	3.760	14.200	11.300	22.033	0.596	35.788	31.568	11.300	30.885	0.973
Sm	1.200	3.570	3.950	5.502	0.227	6.333	7.570	3.950	5.615	0.343
Zr	22.800	85.900	112.000	82.653	6.743	108.038	206.960	112.000	150.059	9.295
Hf	0.719	2.180	3.070	2.103	0.201	3.095	7.414	3.070	4.287	0.265
Eu	0.524	1.110	1.340	1.245	0.098	2.014	2.234	1.340	1.228	0.138
Gd	1.640	3.900	5.550	5.029	0.368	5.274	6.782	5.550	5.130	0.501
Tb	0.310	0.636	1.010	0.789	0.069	0.722	0.998	1.010	0.743	0.092
Dy	2.080	3.980	6.560	4.549	0.503	4.160	4.977	6.560	3.800	0.644
Li	10.000	10.000	14.100	0.000	0.508	12.073	6.730	14.100	0.000	0.653
Y	12.200	23.800	40.700	28.893	3.057	19.975	22.400	40.700	36.769	3.950
Ho	0.461	0.841	1.430	0.988	0.112	0.780	0.766	1.430	0.722	0.143
Er	1.260	2.530	4.090	2.818	0.334	2.025	2.069	4.090	1.750	0.422
Tm	0.195	0.359	0.617	0.429	0.054	0.297	0.261	0.617	0.255	0.066
Yb	1.340	2.470	4.020	2.818	0.373	1.941	1.409	4.020	1.600	0.448
Lu	0.199	0.370	0.636	0.432	0.055	0.283	0.210	0.636	0.250	0.067
$^{87}Sr/^{86}Sr$	0.70350	0.70295	0.70320	0.71121	0.70292	0.70360	0.70354	0.70330	0.70800	0.70500
$^{143}Nd/^{144}Nd$	0.51300	0.51300	0.51302	0.51234	0.51304	0.51280	0.51291	0.51320	0.51240	0.51270
$^{206}Pb/^{204}Pb$	18.5100	18.4200	18.4000	18.8163	17.6000	18.2379	18.0310	17.9000	18.3700	18.4000
$^{207}Pb/^{204}Pb$	15.5800	15.5000	15.4300	15.6941	15.4500	15.5495	15.5090	15.4500	15.5700	15.5700
$^{208}Pb/^{204}Pb$	38.4500	38.2300	37.6000	38.8862	37.5000	38.3790	38.0386	37.6000	38.8000	38.4000

NEJ VF: NE Japan volcanic front, NEJ RA: NE Japan rear arc, SWJ SAB: SW Japan subalkali basalt, SWJ SHO: SW Japan shoshonite, Xn(AOC): NEJ altered oceanic crust, Xn(SED): NEJ sediment, Xn(PERID): NEJ peridotite, Xs(AOC): SWJ altered oceanic crust, Xs(SED): SWJ sediment, Xs(PERID): SWJ peridotite, Note: all trace element compositions are in ppm.

have high distribution coefficients for Rb and K (Green and Adam, 2003). If these are retained in the slab or mantle, excess Rb and K in the calculated basalt can be eliminated. If these minerals break down, increased K and Rb contents in basalt lava can result (Edwards et al., 1991) as exemplified by SWJ shoshonite. We think that these minerals affect K abundances in Japanese arc basalt to some extent but do not exert the most important controls on the compositions of basalts.

DO BULK DISTRIBUTION COEFFICIENTS BETWEEN SLAB AND FLUID AT DIFFERENT PRESSURE–TEMPERATURE CONTROL K-h? – NO

Slab dehydration temperature (T_{slab}) and pressure (P_{slab}) are the major controls of basalt chemistry in the ABS model because distribution coefficients between slab and fluid are sensitive to dehydration P-T conditions, due mainly to combination between difference in residual slab mineralogy and temperature dependent element partitioning. These are due to greater modal garnet content with increasing pressure in residual eclogite and increased distribution coefficients for some elements in fluid with increasing temperature. Such changes occur in slab eclogite consisting of simple quartz-garnet-clinopyroxene-rutile assemblages, and strongly affect element mobilization from the slab to fluids (Kessel et al., 2005a; Sendjaja et al., in press). The lower temperature and pressure expected for the slab beneath the NEJ volcanic front (T_{slab} = 750°C at 5 GPa), greater fractionation of fluid mobile/immobile pairs such as Ba/Th, Pb/LREE, and Sr/LREE occurs in the fluid and these elevated ratios are inherited in the basalt (Fig. 4). Such fractionation is less important for the NEJ rear arc and SWJ magmatic front basalts due to the higher temperatures of dehydration (T_{slab} = 1020-1050°C at P = 4-6 GPa; Figs. 3 and 4). Shallow and deep slab fluids are recognized to have different geochemical and isotopic compositions (Ishizuka et al., 2006; Pearce et al., 1995; Pearce et al., 2005). These differences can be explained by slab dehydration temperature according to the ABS model (Kimura and Yoshida, 2006; Sendjaja et al., in press), and this also explains differences in trace element behavior for arcs subducting hot vs. cold slabs.

TABLE 2. INTENSIVE-EXTENSIVE PARAMETERS ESTIMATED BY THE ABS MODEL CALCULATONS

Model parameters	NE Japan arc		SW Japan arc	
Source peridotite composition	PM	PM	PM	PM
Peridotite depletion (%)	4	4	1	1
Basalts	NEJ VF	NEJ RA	SWJ SAB	SWJ SHO
Slab hybrid AOC/SED fractions				
SED	0.070	0.030	0.030	0.007
AOC	0.930	0.970	0.970	0.993
Slab dehydration temperature/ pressure				
Temperature (°C)	750	1020	1050	1050
Pressure (GPa)	4	6	4	5
Fluid-mantle reaction (zone refining model)				
n	0	1	0.1	0.5
Mantle melting parameter				
Pressure (GPa)	1.0	2.3	2.4	2.4
Melting degree (%)	20	3	5	6
Porosity (%)	1.00	1.00	1.00	1.00
Flux rate (%)	3.00	0.20	0.70	1.20

PM: Primitive mantle of Sun and McDonough (1988); NEJ VF: NE Japan volcanic front; NEJ RA: NE Japan rear arc; SWJ SAB: SW Japan subalkali basalt; SWJ SHO: SW Japan shoshonite; AOC: altered oceacin crust; SED: sediment.

T_{slab} exponentially affects $D_{fluid/solid}$ (Kessel et al., 2005a; Sendjaja et al., in press); therefore, slab dehydration temperature is one of the prime controls of incompatible element abundances in fluids, and via this mechanism, in basalts generated by flux melting. Exceptions are seen for highly fluid-mobile elements (Pearce and Peate, 1995) such as Rb and Pb, which do not have temperature-pressure dependences (Kessel et al., 2005a; Sendjaja et al., in press). Kessel et al. (2005) did not determine $D_{flud/melt}$(K); however, K predictably behaves similar to Rb. Thus, T_{slab} and P_{slab} parameters do not affect K concentrations in basalts and thus is not the most important control of the K-h relationship; nevertheless it is a very important control.

DO SUBDUCTED SEDIMENTS CONTROL K-h? – YES, SLIGHTLY

The composition of subducted oceanic crust and sediments can significantly affect basalt compositions because K is mobile in fluid and silicate melt during slab dehydration and mantle melting (Aizawa et al., 1999; Green, 1994; Green and Adam, 2003; Johnson and Plank, 1999; Kessel et al., 2005a). The SWJ and NEJ subduction zones have different sediment/ igneous crust thickness according to the seismic profiles, 0.5-1 km/ 7-8 km in the NEJ (Miura et al., 2005; Tsuru et al., 2002) and 1.8-3.2 km/ 5.0-6.3 km in SWJ (Kodaira et al., 2002), respectively. Moreover, sediment compositions differ between the two arcs (Table 1). However, estimated X_{SED} components in the slab sources are similar (3-7%, except for shoshonite; Table 2). Slightly elevated K contents in sediments subducted beneath SWJ relative to those subducted beneath NEJ leads to greater K enrichment in calculated SWJ basalt (Table 1, Fig. 4). However, this does not greatly affect the abundances of REE or other trace elements. Such insensitivity is due to the broad similarity of sediment compositions. X_{SED}-X_{AOC} source mass fractions in the ABS model are constrained mainly by Sr-Nd-Pb isotopic compositions. The K contents in the X_{SED} are as much as twice that of X_{AOC} (Fig. 4). A few percent increase in sediment component do not significantly increase K or other incompatible element abundances in the generated basalts. The observed order of magnitude increase in K and incompatible trace elements in the NEJ rear arc basalt relative to that in the volcanic front (Fig. 4) should be attributable to other factors.

DOES FLUID FLUX RATE CONTROL K-h? – YES, BECAUSE IT CONTROLS DEGREE OF MELTING

As indicated by its order of magnitude greater eruption rate (1.94 km^3/Myr/km), the mantle beneath the NEJ volcanic front melts more extensively than does the mantle beneath the rear arc (0.17 km^3/Myr/km) or beneath the SWJ magmatic front (< 0.2 km^3/Myr/km). Although medium-scale (few hundred km) variations in mantle potential temperature are inferred to form "hot fingers" in the mantle wedge (Tamura et al., 2002), there is no indication of significantly hotter mantle beneath NEJ relative to SWJ. Because asthenospheric mantle circulates beneath these different arc segments, it is unlikely that large-scale differences in mantle potential temperature are responsible. Height of the melting column is another possible control (Plank and Langmuir, 1988), but crustal thicknesses everywhere beneath Japan are similar, so this is not likely to

be an important control. The last possibility is fluid fluxing. Addition of H_2O is known to increase the degree of mantle peridotite melting beneath arcs (Hirose and Kawamoto, 1995; Kelley et al., 2006). Therefore, we explore below the likelihood that the extent of melting (F) beneath the arc is principally controlled by the fluid flux rate from the slab into the mantle.

The rate of fluid fluxing into the mantle melting region also affects magma composition, because slab-derived fluids have much higher abundances of fluid-mobile incompatible elements than does mantle peridotite (Kimura and Yoshida, 2006; Sendjaja et al., in press; Fig. 4). The range of F inferred for the Japanese arcs varies from 3% to 20% (Kimura and Yoshida, 2006; Kimura et al., 2005). Higher F is accompanied by decreased abundances of highly incompatible elements in resultant basalts, by as much as an order of magnitude (Fig. 4 and Table 2). Therefore, the effects of increased fluid flux should be examined by total mass balance including β and F parameters.

An interesting correlation exists between NEJ volcanic front and rear arc basalts. ABS suggests that the slab-fluid flux rate (β) in the mantle melting region beneath the volcanic front is ~3% but only ~0.2% beneath the rear arc (note that fluid flux rate expressed by wt.% is almost identical with H_2O wt.% in generated basalt when porosity of the melting system is small enough by the definition of the open system melting calculation (Ozawa and Shimizu, 1995)). Using estimated slab dehydration temperatures of T_{slab} = 750 °C beneath the volcanic front and T_{slab} = 1020 °C beneath the rear arc, then ABS estimates F = 20% beneath the volcanic front and ~3% beneath the rear arc (Table 2). The effect of mantle melting pressure should also be considered, as different melting depths are estimated between the NEJ volcanic front and rear arc (1 GPa beneath the volcanic front vs. 2.3 GPa beneath the rear arc; Table 2; Fig. 6; see also Kimura and Yoshida, 2006). The estimated depths of melting in the mantle wedge, triggered by slab-derived fluids, occur at 2.3-2.4 GPa in both NEJ rear arc and SWJ magmatic front (reference needed). However, a gross positive correlation between flux rate and degree of melting, such as β = 0.2%; F = 3% and β = 1.2%; F = 6% is observed irrespective of the difference in depths of fluid-fluxed melting in the mantle wedge (Table 2, Fig. 6). This again indicates that a greater flux rate leads to increased melting. Although we need to consider mantle P-T conditions, the broad correlation between fluid (H_2O) flux rate and extent of melting holds for both ABS and experimental results. The ABS model results are consistent with an experimentally- determined quasi-linear H_2O-F relationship (Hirose and Kawamoto, 1995) (Fig. 6).

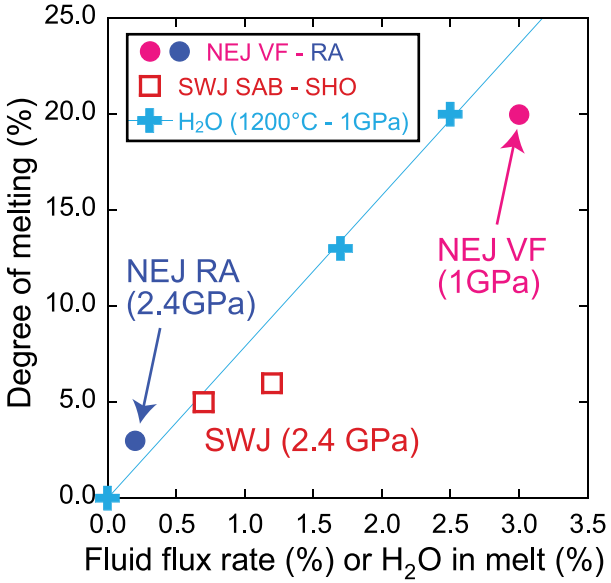

Figure 6. Predicted correlation between fluid flux rate/H_2O in basalt melt and degree of elting of mantle peridotite. Solid cross: experimental results at 1200 °C- 1 GPa (Hirose and Kawamoto, 1995), Red solid circle: ABS model for the NEJ volcanic front (VF) basalt, blue solid circle: ABS model for the NEJ rear arc (RA) basalt, open red squares: SWJ sub-alkali basalt (SAB) and shoshonite (SHO). H_2O in basalt is expressed by fluid flux rate for the ABS model. Fluid flux rate (β) is similar to H_2O in melt (%) in the case of low porosity in the open system melting which we used in our calculations.

We conclude that high fluid flux leads to greater melting, diluting and reducing K and other incompatible elements in arc basalts. Incompatible trace-element abundances are inversely related to the degree of melting (F), which is directly related to fluid flux. Higher flux rate linearly increases F (see Fig. 2 of Hirose and Kawamoto, 1995), in turn, decreasing the incompatible element abundances (see Fig. 14 in Kimura and Yoshida, 2005 for K).

Note that we here use lower T_{slab} (= 750 °C) with greater β (= 3%) to model the NEJ volcanic front, which differs from our previous model T_{slab} = 900 °C with β = 0.7% (Kimura and Yoshida, 2006). We found that T_{slab} and β are compensating parameters that can be adjusted quite a bit and still yield the same model basalt composition. Therefore, fluid flux rate cannot be uniquely constrained by ABS. The 2006 model was constrained using H_2O contents in the primary basalt estimated from olivine melt inclusions (Kimura and Yoshida, 2006) determined to 0.5-1 wt.% elsewhere (Elliott et al., 1997; Kelley et al., 2006). Here we use a 3% H_2O in the primary basalt using the constraint from Hirose and Kawamoto (1995).

Origin of the K-h relationship: Distribution of temperature and fluid in the slab and the mantle wedge

The ABS model explains the K-h relationship for arc lavas. We finally examine 1) the origin of the across-arc variation in the NEJ arc, 2) the origin of the unusual K-h relationship shown by the SWJ arc, and 3) the general control of the K-h relationship globally.

ORIGIN OF THE K-h RELATIONSHIP IN THE NE JAPAN ARC

Based on the previous arguments, we conclude that K concentrations in arc basalts are controlled by both fluid flux rate (β) and melting degree (F). Greater flux rate (3%) is needed to cause more melting (F= 20%) beneath the NEJ volcanic front. Greater fluid flux is suggested not only by the ABS model but also from isotopic studies, such as B, Li, Sr and Pb (Ishikawa and Nakamura, 1994; Ishikawa and Tera, 1999; Moriguti et al., 2004). Therefore, greater fluid flux appears to be the reason that low-K basalts erupt in volcanic arcs that lie above the shallowest parts of most subduction zones, such as the NEJ volcanic front. In contrast, lesser fluid flux in the deep mantle beneath the NEJ rear arc leads to lower degrees of partial melting, resulting in much higher concentrations of highly incompatible elements including K (Fig. 4).

The slab dehydration temperature is expected to be low (750 °C) beneath the NEJ volcanic front and high beneath the NEJ rear arc (1020°C). Such temperature variations control important element ratios, such as Ba/Th and Sr/REE, which also are likely to differ systematically as a function of "h". Such chemical variations are caused by increasing slab dehydration temperature with depth, which in turn indicates that the slab is progressively heated as the slab subducts deeper into the mantle (Hacker and Abers, 2004; Hacker et al., 2003; Peacock et al., 2005; Peacock and Wang, 1999; van Keken et al., 2002). We note that slab temperatures estimated by ABS are high compared to some geodynamic models for NEJ (Furukawa, 1993; Peacock, 1996), but are consistent with recent models that incorporate T-dependent viscosity in the mantle wedge or slab fluid distribution and that indicate higher slab temperature (Kelemen et al., 2003; Peacock et al., 2005; van Keken et al., 2002).

Slab dehydration occurs in response to increased temperature and pressure as the slab subducts. Most slab fluid is released very shallow by increasing pore pressure, allowing escape of water through the porous media. Water contents of slab AOC or sediment can be as much as 20 wt.% (Plank and Langmuir, 1998; Staudigel et al., 1996) but this reduces to ~5 wt.% by ~0.5 GPa (about 15 km depth) by this mechanism (Hacker et al., 2003). Further slab dehydration occurs by prograde-metamorphism due to changing stability of water-bearing minerals. The slab water content gradually decreases to less than 0.5 wt.% by ~3-4 GPa depending on slab temperature (Hacker et al., 2003; Poli and Schmidt, 1995). The slab temperature at these depths is estimated to be between 650 °C and 800 °C for old-cold slab subduction (Peacock et al., 2005; van Keken et al., 2002). This further suggests that intensive slab dehydration beneath magmatic arc is significant beneath the magmatic front area where the Wadati-Benioff Zone lies ~125 km depth (~3 GPa).

WHY UNUSUAL K-h RELATIONSHIP FOR HOT SLAB SUBDUCTION?

SWJ sub-alkali basalt and NEJ rear arc basalt appear to be derived from similar slab temperature (T_{slab} = 1020-1050 °C), fluid flux rate (β = 2-1.2%), mantle melting degree (F = 3-6%), and melting depth (P_{melt} = 2.3-2.4 GPa). These arc segments also are similar in generating an order-of-magnitude less melt than the NEJ volcanic front and in being relatively enriched in K and other incompatible elements. We relate the observed lesser melt in the mantle caused by less fluid flux to the presence of a high temperature subducted slab. Beneath SWJ, the young and hot slab may be less hydrated than old, cold Pacific slab and would reach dehydration temperatures at shallower depths. The fluid budget left in the slab when it reaches a depth where fluids released into the mantle wedge can cause melting is reduced relative to that retained by a cold slab at similar depth. The NEJ RA shows similar behavior, but in this case the fluid flux is reduced because this has largely been lost beneath the volcanic front. Effective dehydration of the slab occurs deeper in the subduction zone for the cold slab, due to the slow increase in slab temperature during subduction (Hacker and Abers, 2004; Hacker et al., 2003; Iwamori, 1998; Peacock et al., 2005; Peacock and Wang, 1999; van Keken et al., 2002). The ABS model indicates that similar slab dehydration temperatures for dehydration beneath the NEJ rear arc and SWJ magmatic front (T_{slab} = 1020-1050 °C) occurs relatively shallow (4 GPa) for SWJ, and deeper (6 GPa) for NEJ (Table 2).

Another reason that the SWJ arc does not have a low-K magmatic front is that mantle convection in the mantle wedge is poorly established due to the shallow angle subduction and recent re-initiation of subduction. Wedge mantle temperatures beneath the Quaternary magmatic front may be similar between NEJ and SWJ even though subducted slab temperatures are different (Peacock and Wang, 1999). The mantle wedge temperature beneath the SWJ forearc is not high enough to melt peridotite even though fluid flux is greater here than beneath the SWJ magmatic arc. Several hot springs with high $^3He/^4He$ are present in the non-magmatic forearc of SWJ, suggesting that slab-derived fluids pass through the mantle wedge without generating melts (Matsumoto et al., 2003; Sano and Wakita, 1985).

FINAL COMMENTS ON THE ORIGIN OF THE K-h RELATIONSHIP

The K-h relationship for most arcs is illuminated by our results for the NEJ arc. The relationship fundamentally reflects different degrees of melting, which in turn are controlled by different rates of fluid flux from the subducting slab beneath the magmatic arc. The maximum fluid flux is achieved by old, cold slabs that retain large amounts of fluid until it is released beneath the volcanic front (e.g., at T_{slab} = 750 °C). Fluids are continuously released from the slab as it subducts and is

conductively heated, until it reaches T_{slab} > 1000 °C beneath the rear arc, at which point it is effectively dehydrated. This model explains the most important part of the K-h correlation found for typical subduction zones.

A new result from our study is that the global K-h relationship is not observed for SWJ and other arcs where young, hot lithosphere is subducted, such as SWJ and Cascade arcs. Instead, a distinct but parallel K-h relation is observed for subduction of young, hot plates, with extremely high K at given h. Such differences are also explained by the ABS model, apparently caused by the fluid flux from hot subducted slab. There may be two reasons for reduced fluid flux from hot slabs; they may not hydrate as extensively as slabs which have a longer cooling history on the seafloor (cold slabs) and they reach effective dehydration temperatures (750-1000 °C) too shallow to trigger significant melting in the mantle wedge. Hot slabs dehydrate relatively shallow, above which overriding mantle wedge temperatures are not high enough to melt. Reduced fluid flux into the mantle wedge beneath the magmatic front generates low-degree melts, high-K basalt with rear arc geochemical signatures (e.g., low Ba/Th and Sr/LREE) along the volcanic front.

CONCLUSIONS

Investigation of magma chemistry using the Arc Basalt Simulator (Sendjaja et al., in press) for the NE Japan old-cold and for the SW Japan young-hot subduction zones provides important insights into the origin of the K-h relationship (Dickinson, 1975; Dickinson and Hatherton, 1967). The temperature of subducted slabs increases with increasing depth, leading to continuous breakdown of hydrous silicate minerals and progressive decrease in slab-derived fluid flux. Continuous decrease in fluid flux with depth causes decreased partial melting of the mantle wedge beneath the rear arc, leading to systematically higher K contents with depth and thus the K-h relationship. We conclude that the slab thermal structure is the fundamental cause of the K-h relationship, because it controls fluid flux into the mantle wedge. The global K-h relationship is violated for young-hot subduction zones, which erupt more potassic lavas at shallower slab depths. This anomalous behavior is also controlled by slab temperature. Young, hot subducted slabs release fluids shallower than do old, cold subducted slabs. In the hot slab case, fluids are lost where the superjacent mantle is not hot enough to melt, whereas cold slabs lose water deep enough to affect overlying mantle that is hot enough to melt. Similar trace element compositions between rear arc volcanoes of old-cold subduction zones and those of the volcanic front above young-hot subduction further supports this explanation because the trace element composition of inferred slab fluids for both situations indicate high temperature dehydration. Analysis using the ABS model is thus quite useful for identifying the most important magma genetic processes operating beneath magmatic arcs. With this, we propose that the significance of the K-h relationship be studied further, along with the considerations of geophysics and geochemistry of the mantle wedge beneath arcs.

We conclude that temperature and fluid distributions in the subducting slab and mantle wedge primarily control both the chemistry of slab-derived fluids and melting of the mantle and explains the most important part of the K-h relationship. We also conclude that the elegant K-h relationship proposed by Dickinson and co-workers (Dickinson, 1975; Dickinson and Hatherton, 1967) still provides important insights into how arc magmas are generated.

ACKNOWLEDGMENTS

We appreciate discussions with Prof. T. Yoshida of Tohoku University, Japan on the way to create the ABS model. Analyses of the SWJ lavas were performed by Mr. Y. Shimoshioiri and Ms. M. Katakuse of Shimane University. Reviews by Drs. J.E. Spencer and J.B. Gill were very useful in improving the clarity of the manuscript.

REFERENCES CITED

Aizawa, Y., Tatsumi, Y., and Yamada, H., 1999, Element transport by dehydration of subducted sediments: Implications for arc and ocean island magmatism: The Island Arc, v. 8, p. 38-46.

Aramaki, S., and Ui, T., 1982, Japan, *in* Thorpe, R. S., ed., Andesites: Chichester, John Wiley & Sons, p. 259-292.

Ayers, J., 1998, Trace element modeling of aqueous fluid - peridotite interaction in the mantle wedge of subduction zones: Contributions to Mineralogy and Petrology, v. 132, p. 390-404.

Clift, P., and Vannucchi, P., 2004, Controls on tectonic accretion versus erosion in subduction zones: Implications for the origin and recycling of the continental crust: Reviews of Geophysics, v. 42, p. doi:10.1029/2003RG000127.

Coats, R. R., 1962, Magma type and crustal structure in the Aleutian arc: American Geophysical Union Monograph v. 6, p. 92-109.

Dickinson, W. R., 1975, Potash-depth (K-h) relations in continental margins and intra-oceanic magmatic arcs: Geology, v. 3, p. 53-56.

Dickinson, W. R., and Hatherton, T., 1967, Andesitic volcanism and seismicity around the Pacific: Science, v. 157, p. 801.

Edwards, C. M. H., Menzies, M. A., and Thirlwall, M. F., 1991, Evidence from Muriah, Indonesia, for the interplay of suprasubduction zone and intraplate processes in the genesis of potassic alkaline magmas: Journal of Petrology, v. 32, p. 555-592.

Elliott, T., Plank, T., Zindler, A., White, W., and Bourdon, B., 1997, Element transport from slab to volcanic front at the Mariana arc: Journal of Geophysical Research, v. 102, p. 14,991-15,019.

Furukawa, Y., 1993, Magmatic processes under arcs and formation of the volcanic front: Journal of Geophysical Research, v. 98, p. 8309-8319.

GEOROC, 2007, Geochemistry of rocks of the oceanc and the continents: Max-Planck-Institut für Chemie, accessed 2008 at http://georoc.mpch-mainz.gwdg.de/georoc/.

Gill, J. B., 1981, Orogenic andesites and plate tectonics: Heidelberg, Springer-Verlag, 385 p.

Green, T. H., 1994, Experimental studies of trace-element partitioning applicable to igneous petrogenesis - Sedona 16 years later: Chemical Geology, v. 117, p. 1-36.

Green, T. H., and Adam, J., 2003, Experimentally-determined trace element characteristics of aqueous fluid from partially dehydrated mafic oceanic crust at 3.0 GPa, 650-700° C: European Journal of Mineralogy, v. 15, p. 815-830.

Hacker, B. R., and Abers, G. A., 2004, Subduction factory 3: An EXCEL worksheet and macro for calculating the densities, seismic wave speeds, and H_2O contents of minerals and rocks at pressure and temperature: Geochemistry Geophysics Geosystems (G3), v. 5, p. doi:10.1029/2003GC000614.

Hacker, B. R., Abers, G. A., and Peacock, S. M., 2003, Subduction factory 1. Theoretical mineralogy, densities, seismic wave speeds, and H_2O contents: Journal of Geophysical Research, v. 108, p. doi:10.1029/2001JB001127.

Hasegawa, A., Zhao, D., Hori, S., Yamamoto, A., and Horiuchi, S., 1991, Deep structure of the northeastern Japan arc and its relationship to seismic and volcanic activity: Nature, v. 352, p. 683-689.

Hatherton, T., and Dickinson, W. R., 1969, The relationship between andesitic volcanism and seismicity in Indonesia: Journal of Geophysical Research, v. 74, p. 5301-5310.

Hauff, F., Hoernle, K., and Schmidt, A., 2003, Sr-Nd-Pb composition of Mesozoic Pacific oceanic crust (Site 1149 and 801, ODP Leg 185): Implications for alteration of ocean crust and the input into the Izu-Bonin-Mariana subduction system: Geochemistry Geophysics Geosystems, v. 4, p. doi:10.1029/2002GC000421.

Hickey-Vargas, R., 1991, Isotope characteristics of submarine lavas from the Philippine Sea: implications for the origin of arc and basin magmas of the Philippine tectonic plate: Earth and Planetary Science Letters, v. 107, p. 290-304.

Hickey-Vargas, R., 1998, Origin of the Indian Ocean-type isotopic signature in basalts from Philippine Sea plate spreading centers: An assessment of local versus large-scale processes: Journal of Geophysical Research, v. 103, p. 20,963-20,979.

Hickey-Vargas, R., Hergt, J. M., and Spadea, P., 1995, The Indian Ocean-type isotopic signature in Western Pacific marginal basins: Origin and significance, *in* Taylor, B., and Natland, J., eds., Active Margins and Marginal Basins of the Western Pacific: Washinton DC, American Geophysical Union, p. 175-197.

Hirose, K., and Kawamoto, T., 1995, Hydrous partial melting of lherzolite at 1 Gpa: The effect of H_2O on the genesis of basaltic magmas: Earth and Planetary Science Letters, v. 133, p. 463-473.

Hoang, N., and Uto, K., 2003, Geochemistry of Cenozoic basalts in the Fukuoka district (northern Kyushu, Japan): Implications for asthenosphere and lithospheric mantle interaction: Chemical Geology, v. 198, p. 249-268.

Hochstaedter, A., Gill, J., Peters, R., Broughton, P., Holden, P., and Taylor, B., 2001, Across-Arc Geochemical trends in the Izu-Bonin Arc: Contributions from the Subducting Slab: Geochemistry, Geophysics, Geosystems (G3), v. 2, n. 7, doi:10.1029/2000GC000105.

Hutchison, C. S., 1982, Indonesia, *in* Thorpe, R. S., ed., Andesites: Chicester, John Wiley & Sons, p. 207-224.

Ishikawa, T., and Nakamura, E., 1994, Origin of the slab component in arc lavas from across-arc variation of B and Pb isotopes: Nature, v. 370, p. 205-208.

Ishikawa, T., and Tera, F., 1999, Two isotopically distinct fluid components involved in the Mariana Arc: evidence from Nb/B ratios and B, Sr, Nd, and Pb isotope systematics: Geology, v. 27, p. 83-86.

Ishizuka, O., Taylor, R. N., Milton, J. A., and Nesbitt, R. W., 2003, Fluid-mantle interaction in an intra-oceanic arc: constraints from high-precision Pb isotopes: Earth and Planetary Science Letters, v. 211, p. 221-236.

Ishizuka, O., Taylor, R. N., Milton, J. A., Nesbitt, R. W., Yuasa, M., and Sakamoto, I., 2006, Variation in the mantle sources of the northern Izu arc with time and space - Constraints from high-precision Pb isotopes: Journal of Volcanology and Geothermal Research, v. 156, p. 266-290.

Iwamori, H., 1998, Transport of H_2O in subduction zones: Earth and Planetary Science Letters, v. 160, p. 65-80.

Johnson, M. C., and Plank, T., 1999, Dehydration and melting experiments constrain the fate of subducted sediments: Geochemistry Geophysics Geosystem (G3), v. 13, n. 1, doi:10.1029/1999GC000014.

Kelemen, P. B., Rilling, J. L., Parmentier, E. M., Mehl, L., and Hacker, B. R., 2003, Thermal structure due to solid-state flow in the mantle wedge beneath arcs, *in* Eiler, J., ed., Inside the Subduction Factory: Geophysical Monograph: Washington D.C., American Geophysical Union, p. 293-311.

Kelley, K. A., Plank, T., Grove, T. L., Stolper, E. M., Newman, S., and Hauri, E., 2006, Mantle melting as a function of water content beneath back-arc basins: Journal of Geophysical Research, v. 111, p. doi:10.1029/2005JB003732.

Kelley, K. A., Plank, T., Ludden, J., and Staudigel, H., 2003, Composition of altered oceanic crust at ODP Sites 801 and 1149: Geochemistry Geophysics Geosystems, v. 4, p. doi:10.1029/2002GC000435.

Kessel, R., Schmidt, M. W., Ulmer, P., and Pettke, T., 2005a, Trace element signature of subduction-zone fluids, melts and supercritical liquids at 120-180 km depth: Nature, v. 439, no. 724-727.

Kessel, R., Ulmer, P., Pettke, T., Schmidt, M. W., and Thompson, A. B., 2005b, The water-basalt system at 4 to 6 GPa: Phase relations and second critical endpoint in a K-free eclogite at 700 to 1400° C: Earth and Planetary Science Letters, v. 237, p. 873-892.

Kimura, J.-I., Manton, W. I., Sun, C.-H., Iizumi, S., Yoshida, T., and Stern, R. J., 2001, Chemical diversity of the Ueno Basalts, central Japan: Identification of mantle and crustal contributions to arc basalts: Journal of Petrology, v. 43, p. 1923-1946.

Kimura, J.-I., Nagao, T., Yamauchi, S., Kakubuchi, S., Okada, S., Fujibayashi, N., Okada, R., Murakami, H., Kusano, T., Umeda, K., Hayashi, S., Ishimaru, T., Ninomiya, J., and Tanase, A., 2003, Late Cenozoic volcanic activity in the Chugoku area, Southwest Japan arc during back arc basin opening and re-initiation of subduction: The Island Arc, v. 12, p. 22-45.

Kimura, J.-I., Stern, R. J., and Yoshida, T., 2005, Re-initiation of subduction and magmatic responces in SW Japan during Neogene time: Geological Society of America Bulletin, v. 117, p. 969-986.

Kimura, J.-I., and Yoshida, T., 2005, Mass balance of the arc: Implications from Quaternary volcanic rocks in the NE Honshu arc, Japan: Earth Monthly, v. 52, p. 34-38.

Kimura, J.-I., and Yoshida, T., 2006, Contributions of slab fluid, mantle wedge and crust to the origin of Quaternary lavas in the NE Japan arc: Journal of Petrology, v. 47, p. 2185–2232.

Kodaira, S., Kurashimo, E., Park, J.-O., Takahashi, N., Nakanishi, A., Miura, S., Iwasaki, T., Hirata, N., Ito, K., and Kaneda, Y., 2002, Structural factors controlling the rupture process of a megathrust earthquake at the Nankai trough seismogenic zone: Geophysical Journal International, v. 149, p. 815–835.

Kuno, H., 1966, Lateral variation of basalt magma type across continental margin and island arcs: Bulletin Volcanologique, v. XXIX, p. 195-222.

Leeman, W. P., Lewis, J. F., Evarts, R. C., Conrey, R. M., and Streck, M. A., 2005, Petrologic constraints on the thermal structure of the Cascades arc: Journal of Volcanology and Geothermal Research v. 140, p. 67–105.

Matsumoto, T., Kawabata, T., Matsuda, J., Yamamoto, K., and Mimura, K., 2003, $^{3}He/^{4}He$ ratios in well gases in the Kinki district, SW Japan: surface appearance of slab-derived fuids in a non-volcanic area in Kii Peninsula: Earth and Planetary Science Letters, v. 216, p. 221-230.

Maumus, J., Laporte, D., and Schiano, P., 2004, Dihedral angle measurements and infiltration property of SiO_2-rich melts in mantle peridotite assemblages: Contributions to Mineralogy and Petrology, v. 148, p. 1-12.

Miura, S., Takahashi, N., Nakanishi, A., Tsuru, T., Kodaira, S., and Kaneda, Y., 2005, Structural characteristics off Miyagi forearc region, the Japan Trench seismogenic zone, deduced from a wide-angle reflection and refraction study: Tectonophysics, v. 407, p. 165– 188.

Moriguti, T., Shibata, T., and Nakamura, E., 2004, Lithium, boron and lead isotope and trace element systematics of Quaternary basaltic volcanic rocks in northeastern Japan: mineralogical controls on slab-derived fluid composition: Chemical Geology, v. 212, p. 81-100.

Morris, P. A., 1995, Slab melting as an explanation of Quaternary volcanism and aseismicity in southwest Japan: Geology, v. 23, p. 395-398.

Nakajima, J., and Hasegawa, A., 2007, Subduction of the Philippine Sea plate beneath southwestern Japan: Slab geometry and its relationship to arc magmatism: Journal of Geophysical Research, v. 112, p. doi:10.1029/2006JB004770, 2007.

Nakajima, J., Takei, Y., and Hasegawa, A., 2005, Quantitative analysis of the inclined low-velocity zone in the mantle wedge of northern Japan: A systematic change of melt-filled pore shapes with depth and its implications for melt migration: Earth and Planetary Science Letters, v. 234, p. 59-70.

Nakanishi, M., Tamaki, K., and Kobayashi, K., 1992, Magnetic anomaly lineations from Late Jurassic to Early Cretaceous in the west-central Pacific Ocean: Geophysical Journal International, v. 109, p. 701-719.

Ochi, F., Nakamura, M., and Zhao, D., 2001, Deep structure of the subducting Philippine Sea slab under southwestern Japan: Earth Monthly, v. 23, p. 679– 684.

Okino, K., Shimakawa, Y., and Nagaoka, S., 1994, Evolution of the Shikoku Basin: Journal of Geomagnetism and Geoelectricity, v. 46, p. 463-479.

Ozawa, K., and Shimizu, N., 1995, Open-system melting in the upper mantle: Constraints from the Hayachine-Miyamori ophiolite, northeastern Japan: Journal of Geophysical Research, v. 100, p. 22,315-22,335.

Peacock, S. M., 1996, Thermal and Petrologic Structure of Subduction Zones, *in* Bebout, G. E., Scholl, D. W., Kirby, S. H., and Platt, J. P., eds., Subduction: Top to Bottom: Washington DC, American Geophysical Union, p. 119-133.

Peacock, S. M., van Keken, P. E., Hollowey, S. D., Hacker, B. R., Abers, G. A., and Fergason, R. L., 2005, Thermal structure of the Costa Rica - Nicaragua subduction zone: Physics of the Earth and Planetary Interiors, v. 149, p. 187-200.

Peacock, S. M., and Wang, K., 1999, Seismic consequence of warm versus cool subduction metamorphism: Examples from southwest and northeast Japan: Science, v. 286, p. 937-939.

Pearce, J. A., 2005, Mantle preconditioning by melt extraction during flow: Theory and petrogenetic implications: Journal of Petrology, v. 46, p. 973-997.

Pearce, J. A., Baker, P. E., Harvey, P. K., and Luff, I. W., 1995, Geochemical evidence for subduction fluxes, mantle melting and fractional crystallization beneath the South Sandwitch Island arc: Journal of Petrology, v. 36, p. 1073-1109.

Pearce, J. A., and Parkinson, I. J., 1993, Trace element models for mantle melting: application to volcanic arc petrogenesis, *in* Prichard, H. M., Alabaster, T., Harris, N. B. W., and Neary, C. R., eds., Magmatic Processes and Plate Tectonics: London, Geological Society Special Publication, p. 373-403.

Pearce, J. A., and Peate, D. W., 1995, Tectonic implications of the composition of volcanic arc magmas: Annual Review in Earth and Planetary Sciences, v. 23, p. 251-285.

Pearce, J. A., Stern, R. J., Bloomer, S. H., and Fryer, P., 2005, Geochemical mapping of the Mariana arc-basin system: Implications for the nature and distribution of subduction components: Geochemistry Geophysics Geosystems, v. 7, p. doi:10.1029/2004GC000895.

Plank, T., and Langmuir, C. H., 1998, The chemical composition of subducting sediment and its consequence for the crust and mantle: Chemical Geology, v. 145, p. 325-394.

Poli, S., and Schmidt, M. W., 1995, H_2O transport and release in subduction zones: Experimental constraints on basaltic and andesitic systems: Journal of Geophysical Research, v. 100B, p. 22299-22314.

Sakuyama, M., and Nesbitt, R. W., 1983, Geochemistry of the Quaternary volcanic rocks of the Northeast Japan arc: Journal of Volcanology and Geothermal Research, v. 29, p. 413-450.

Sano, Y., and Wakita, H., 1985, Geographical distribution of $^{3}He/^{4}He$ ratios in Japan: Implications for arc tectonics and incipient magmatism: Journal of Geophysical Research, v. 90, p. 8729-8741.

Sendjaja, Y.A., Kimura J.-I., and Sunardi, E., *in press*, Across-arc geochemical variation of Quaternary lavas in West Java, Indonesia: Mass-balance elucidation using the Arc Basalt Simulator model: Island Arc.

Seno, T., Stein, S., and Gripp, A. E., 1993, A model for the motion of the Philippine Sea Plate consistent with NUVEL-1 and geological data: Journal of Geophysical Research, v. 98, no. B10, p. 17,941-17,948.

Shibata, T., and Nakamura, E., 1997, Across-arc variations of isotope and trace element compositions from Quaternary basaltic rocks in northeastern Japan: Implications for interaction between subducted oceanic slab and mantle wedge: Journal of Geophysical Research, v. B102, p. 8051-8064.

Shimoda, G., Tatsumi, Y., Nohda, S., Ishizaka, K., and Jahn, B. M., 1998, Setouchi high-Mg andesites revisited: geochemical evidence for melting of subducting sediments.: Earth and Planetary Science Letters, v. 160, p. 479-492.

Staudigel, H., Plank, T., White, B., and Schmincke, H.-U., 1996, Geochemical fluxes during seafloor alteration of the basaltic upper crust: DSDP Sites 417 and 418: Geophysical Monograph, v. 96, p. 19-38.

Stern, R. J., 2002, Subduction zones: Reviews of Geophysics, v. 40, p. 1012, doi:1029/2001RG000108.

Sun, S.-s., and McDonough, W. F., 1989, Chemical and isotopic systematics of oceanic basalts: implications for mantle composition and processes: Geological Society Special Publication, v. 42, p. 313-345.

Taira, A., 2001, Tectonic evolution of the Japanese island arc system: Annual Review in Earth and Planetary Sciences, v. 29, p. 109-134.

Tamura, Y., Tani, K., Chang, Q., Shukuno, H., Kawabata, H., Ishizuka, O., and Fiske, S., 2007, Wet and dry basalt magma evolution at Torishima volcano, Izu-Bonin arc, Japan: the possible role of phengite in the downgoing slab: Journal of Petrology, v. 48, p. 1999-2031.

Tatsumi, Y., and Eggins, S., 1995, Subduction zone magmatism: Massachusetts, Blackwell Science, 211 p.

Tatsumi, Y., and Hanyu, T., 2003, Geochemical modeling of dehydration and partial melting of subducting lithosphere: Toward a comprehensive understanding of high-Mg andesite formation in the Setouchi volcanic belt, SW Japan: Geochemistry Geophysics Geosystems (G3), v. 4, n. 9, doi: 10.1029/2003GC000530.

Tatsumi, Y., Ishikawa, N., Aono, K., Ishizaka, K., and Itaya, T., 2001, Tectonic setting of high-Mg andesite magmatism in the SW Japanarc: K-Ar chronology of the Setouchi volcanic belt: Geophysics International, v. 144, p. 625-631.

Tiepolo, M., Vannucci, R., Oberi, R., Foley, S., Bottazzi, P., and Zanetti, A., 2000, Nb and Ta incorporation and fractionation in titanian pargasite and kaersutite: Crystal-chemical constraints and implications for natural systems: Earth and Planetary Science Letters, v. 176, p. 185-201.

Tsuru, T., Park, J.-O., Miura, S., Kodaira, S., Kido, Y., and Hayashi, T., 2002, Along-arc structural variation of the plate boundary at the Japan Trench margin: Implication of interplate coupling: Journal of Geophysical Research, v. 107, doi:10.1029/2001JB001664.

van Keken, P. E., Kiefer, B., and Peacock, S. M., 2002, High resolution models of subduction zones: Implications for mineral dehydration reactions and the transport of water into the deep mantle: Geochemistry Geophysics Geosystems (G3), v. 3, doi:10.1029/2001GC000256.

von Huene, R., and Scholl, D. W., 1991, Observations at convergent margins concerning sediment subduction, subduction erosion, and the growth of continental crust: Reviews of Geophysics, v. 29, p. 279–316.

White, R. S., McKenzie, D. P., and O'Nions, R. K., 1992, Oceanic crustal thickness from seismic measurements and rare earth element inversions: Journal of Geophysical Research, v. 97, p. 19 683–19 715.

Zou, H., 1998, Trace element fractionation during modal and nonmodal dynamic melting and open-system melting: A mathematical treatment: Geochimica et Cosmochimica Acta, v. 62, p. 1937-1945.

Zou, H., 1999, Erratum to Zou H. (1998) "Trace element fractionation during modal and nonmodal dynamic melting and open-system melting: A mathematical treatment" Geochimica et Cosmochimica Acta 62, 1937-1945: Geochimica et Cosmochimica Acta, v. 63, p. 2695.